Available online at www.sciencedirect.com
ScienceDirect
Engineering Geology 91 (2007) 4–15
ENGINEERING GEOLOGY
www.elsevier.com/locate/enggeo

Influence of earthquakes on the stability of slopes

Robert Hack [a,*], Dinand Alkema [b,1], Gerard A.M. Kruse [c,2], Noud Leenders [d,3], Lucia Luzi [e,4]

[a] *Engineering Geology, Earth Systems Analysis, International Institute for Geo-Information Science and Earth Observation (ITC), Hengelosestraat 99, P.O. Box 6, 7500 AA Enschede, The Netherlands*
[b] *Earth Systems Analysis, International Institute for Geo-Information Science and Earth Observation (ITC), P.O. Box 6, 7500 AA Enschede, The Netherlands*
[c] *Geodelft, P.O. Box 69, 2600 AB Delft, The Netherlands*
[d] *Private Mail Bag, GPO, Suva, Fiji Islands, Street Address: Mead Road, Nabua, Fiji*
[e] *Istituto Nazionale di Geofisica e Vulcanología, Sezione di Milano, via Bassini 15, 20133, Milano, Italy*

Accepted 11 December 2006
Available online 26 January 2007

Abstract

Earthquakes are a major trigger for instability of natural and man-made slopes. Often the instability of slopes due to an earthquake causes more destruction and kills more people than the actual earthquake itself. A comparison is made between different methodologies to analyze the potential stability of slopes during earthquakes. Theoretically, it seems simple to calculate the stability of a slope during an earthquake. In reality, however, the stability is influenced by so many parameters that are either not known or which influence is so poorly known that a decent estimation of stability cannot be made. Offshore the situation is worse because proper data required for stability calculations are even less available than onshore. On- and offshore, erosion and weathering create continuously slopes that may become unstable during a future earthquake, offshore also sedimentation creates continuously new slopes. Another fundamental problem in stability analysis is the complicated and largely unknown behavior of seismic waves in three-dimensions in natural materials. The lack of accurate data and the unknown behavior of seismic waves in three-dimensions make estimations of slope stability during an earthquake unreliable.

Keywords: Slope; Stability; Earthquake; Crocodile; Armenia; Roermond; Umbria–Marche

1. Introduction

Earthquakes have a determining and clear influence on slope stability. This is already clear in ancient times. The Bible's account of the destruction of Sodom and Gomorrah may partly be attributed to an earthquake triggered liquefaction and subsequent landslide that swept the cities into the Death Sea (Harris and Beardow, 1995). More recently, the magnitude 7.5 Guatemala Earthquake of 1976 is reported to have generated at least 10,000 landslides and slope failures (Anon, 1997). The slope instabilities and resulting disasters after the El Salvador Earthquakes in 2001 hit the front pages of the

* Corresponding author. Tel.: +31 53 4874444, +31 6 24505442; fax: +31 53 48744400.
E-mail addresses: hack@itc.nl (R. Hack), alkema@itc.nl (D. Alkema), kru@geodelft.nl (G.A.M. Kruse), Noud@sopac.org (N. Leenders), lucia.luzi@mi.ingv.it (L. Luzi).
[1] Tel.: +31 53 4874444; fax: +31 53 48744400.
[2] Tel.: +31 15 2693728; fax: +31 15 2610821.
[3] Tel.: +679 338 1377, +679 9999388 (Mob); fax: +679 337 0040.
[4] Tel.: +39 02 23699285; fax: +39 02 23699458.

0013-7952/$ - see front matter © 2007 Elsevier B.V. All rights reserved.
doi:10.1016/j.enggeo.2006.12.016

papers worldwide. Offshore, sub-marine and in lakes, slope failures during earthquakes do not normally make the world news, except if onshore structures are damaged due to major tsunamis resulting from slope instability. A recent example is the forecast of the instability of a large part of the Canary Island "La Palma" that if it fails would cause a destructive tsunami in the countries bordering the Atlantic Ocean. The importance of smaller-scale slope stability during earthquakes is obvious for offshore structures, such as oil industry platforms.

Natural and artificial slopes may become equally unstable during an earthquake. The earthquake triggers the failure, but is virtually never the cause of the failure. Weathering, erosion and sedimentation that reduce the strength of the sub-surface soil or rock masses or changes the geometry of a slope, and man-made influences, such as road cuts or agricultural use on a slope, are normally the cause for a failed slope during an earthquake. To calculate how a slope will behave during an earthquake or to design a slope that is also stable under earthquake conditions is not that easy. A considerable amount of research work has been done in recent years to establish design parameters for slopes under the influence of an earthquake. These studies consider laboratory simulations of scale models of slopes on shaking tables or in centrifuges as well as back analyses of existing slopes (among others Boulanger et al., 1995; Hatzor and Goodman, 1997; Nova-Roessig and Sitar, 1998; Rathje and Bray, 2001). The results are presented in the proceedings of numerous conferences on earthquakes, among others the series of conferences "Recent Advances in Geotechnical Earthquake Engineering and Soil Dynamics" (Prakash, 2001). Another line of research has been to improve the ability to forecast the stability of slopes over larger areas (among others Khazai and Sitar, 2000; Slob et al., 2002).

In this paper an overview is given of some recent work in which Jan Nieuwenhuis was involved in which failed slopes are analyzed to obtain better parameters to design future slopes.

1.1. Pseudostatic slope stability analyses

The pseudostatic, simple standard calculation of slope stability under influence of an earthquake is given in Fig. 1 for a slope in a discontinuous rock mass (e.g. a slope in a rock mass that includes planes of weakness such as bedding planes, joints, etc.).

The safety factor is calculated following:

$$F = \frac{\text{resisting stresses}}{\text{driving stresses}} = \frac{\text{coh} + ((W-\beta W)\cos\psi - \alpha W \sin\psi - u) * \tan\varphi}{(W-\beta W)\sin\psi + \alpha W \cos\psi + v\cos\psi} \quad (1)$$

coh, φ = cohesion, respectively friction along discontinuity
W = weight of block; u, v are the water pressures in the discontinuities
$\alpha W, \beta W$ = horizontal and vertical acceleration due to an earthquake

Vertical acceleration is often neglected and, generally, only horizontal peak acceleration is considered. During the earthquake, the horizontal acceleration adds an unfavorably oriented force to the blocks that may cause instability. However, the acceleration also reduces normal stresses on the contact plane and thereby the contribution of the friction to the shear strength along the plane. The contribution of the cohesion to the shear strength may be real cohesion due to cementation or apparent cohesion due to asperities on the discontinuity plane. During an earthquake, the cementation may be broken, asperities may be broken, or asperities may be overridden leading to non-fitting roughness patterns, all resulting in a cohesion and friction that are permanently reduced. Hence, an earthquake does not only add unfavorable forces to a slope but may also permanently reduce the shear strength along the discontinuity planes in a slope.

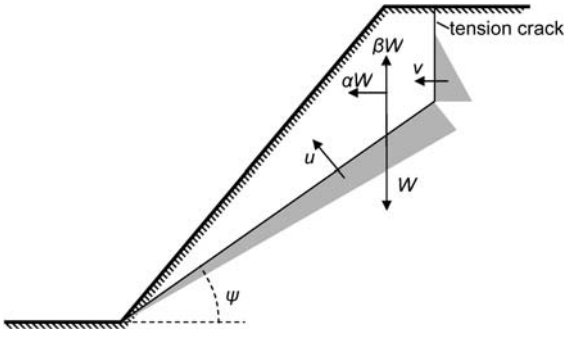

Fig. 1. Pseudostatic slope stability analysis; stresses working on a block of rock with tension crack on a sliding plane and during an earthquake. The discontinuity is free draining at the toe of the slope.

1.2. Soil slopes under influence of an earthquake

Similar calculations and effects are obtained in slopes in soil masses. In a soil slope the slope stability may decrease in three ways:

- Ground acceleration due to seismic waves adds to the destabilizing forces on the soil mass,
- Where tensile strength between the soil particles exists (for example due to cementation), ground displacements due to seismic waves may be sufficiently large to rupture bonds between soil particles, leading to loss of tensile strength and cohesion (Ishihara, 1986),
- Seismic waves cause a cyclic loading effect on the soil. In loose unconsolidated soils, this may lead to compaction thereby reducing pore volume. If the pore water cannot drain fast enough, the pore pressure will increase, the effective stresses between the grains will be reduced, and, hence the shear strength between the grains will be reduced. Eventually, the soil may lose all its shear strength and the soil may liquefy. On slopes failure will occur before the shear strength is reduced to zero. An extensive overview of the mechanics of fluid-filled porous solids is given by Hubbert and Rubey (1959).

An earthquake generally consists of series of cycles of horizontal and vertical acceleration. The pseudostatic calculation in Eq. (1) does not consider this. The slope and the blocks on the slope may well be in resonance with the tremor and this may cause that the slope is unstable even in situations where a pseudostatic calculation would result in a stable slope (Terzaghi, 1950).

Newmark (1965) extended the pseudostatic analyses and introduced the criterion of displacement rather than stress equilibrium. This results in stability calculations that are dependent on the length of time that an accelerated stress exceeds the resisting stresses and on the amplitude and frequency of the acceleration cycles. Further more sophisticated analyze methodologies became possible when computers allowed the calculation of dynamic numerical programs that will numerically calculate the behavior of a slope under influence of an earthquake.

1.3. Seismic wave behavior

Although the simple mechanical models are easy to understand, the simple mechanical models are often not enough to explain the observed instabilities. It is necessary to understand the behavior of seismic waves in inhomogeneous and anisotropic materials to understand the results. However, to translate this into a calculation on slope stability is often impossible because accurate data on properties is missing.

The seismic wave creating the shock at the location travels via the fastest route, e.g. generally this is the bedrock below the weathered top layers of the bedrock and below the topsoil layer. The weathered material and topsoil move with the displacements in the bedrock. However, the particle velocity at surface will be larger than at bedrock level because of the smaller stiffness (thus lower seismic velocities) and density of the weathered and topsoil materials. This behavior contributes to the geotechnical amplification or 'site effect'. The amount of amplification is dependent on frequency (Fig. 2).

In slopes other effects will also occur. The slope face forms the boundary between the ground material and air. The slope face will act as a boundary for the seismic wave and most of the energy of a seismic wave is reflected on the slope face. The reflected waves will interfere with the incident waves. A second effect is that at the boundary virtually no further resistance against displacement exists (there is "air" past the boundary) with result that the displacements at the slope face will be larger. Along with site effects described above the behavior of the slope during the passing of a seismic wave becomes highly complex.

1.4. Probabilistic slope stability analyses

In most areas, not enough data of the sub-surface materials or of the seismic wave are available to allow for a detailed deterministic calculation of slope stability. Alternatively, a type of stochastic probability approach can be used to establish a series of rules or empirical relations that will indicate slope stability problems that can be expected during an earthquake with certain characteristics. Factors that are generally included in such empirical probabilistic approaches are the slope dip; shaking severity; strength and engineering properties of geologic materials; water saturation, existing landslide areas; and vegetation cover.

1.5. Offshore slope stability

Slope stability related to earthquake loading offshore differs from on land in several ways. Whereas notably erosion changes the loading conditions for slopes on land, erosion and sedimentation together are the main

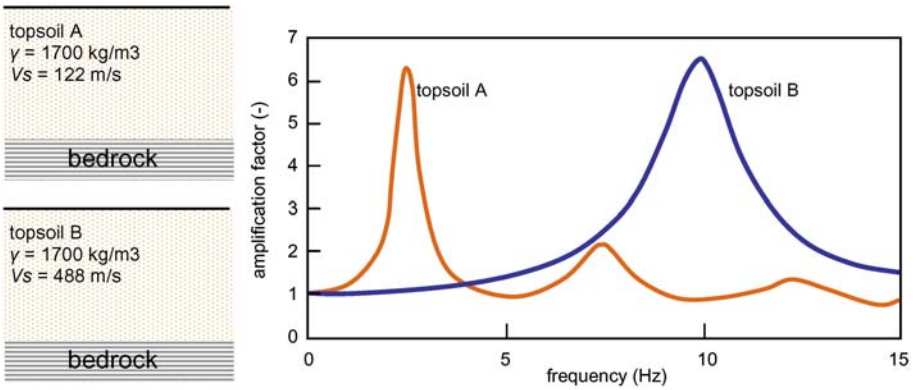

Fig. 2. Amplification due to lower stiffness of topsoil layers (topsoil is assumed to be linearly elastic and bedrock is rigid; γ = density of material and Vs is the shear wave velocity) (free after Kramer, 1996).

factors for changing offshore slope stability. Pore pressure fluctuations on land due to changing weather, topography, and vegetation do not occur as such offshore, but compaction due to continuous sedimentation and methane generation is involved in pore pressure changes offshore. Also the early diagenetic changes in soil and weathering profile development do not occur as such in offshore areas, instead the early diagenetic changes tend to increase the strength of initially generally weak offshore soils. Only in regions of high tectonic activity, or of extreme Pleistocene glacial erosion, bedrock like materials can become involved locally. In offshore conditions, human interference apart from dredging rarely causes increase in regional slope stability hazards, contrary to on land regions where i.e. deforestation can increase the hazard significantly. Long-term anthropogenic global changes, such as climatic change, have far less effect on offshore slope stability compared to on land.

As with on land conditions, zones in offshore regions with significant slopes and slope stability issues can be well delineated. The prominent offshore zones of stability issues in order of frequency are:

- Continental slopes, the most widespread zone of stability issues;
- The zones of intense tectonic deformation related to subduction and rifting, often combined with emerging continental slopes;
- Zones of intense sedimentation in deltaic regions;
- The slopes of deeply eroded valleys in formerly glaciated areas.

In many places on earth the continental slopes experience, at least a somewhat increased seismic activity, and the subduction and rifting zones are notorious for their seismic activity. It should be noted that slopes with a dip less than 5° already can be pocked with scars due to the very weak nature of the materials in much of the offshore terrain.

Since observation of material characteristics in offshore regions is complicated, a considerable amount of uncertainty exists on the spatial distribution of the deformation, mass density and hydraulic permeability properties of materials involved at a specific location. Even generation of typical sections for slope stability analyses requires large uncertainties to be taken into account. Assessing slope stability hazard under earthquake loading therefore has increased uncertainties compared to such hazard evaluation on land.

As is the case on land, it is easy to identify the scars of slope failures, but detailed bathymetric and shallow seismic surveys offshore are required to comprehend the stability of slopes. Determining the conditions forming the scars is however complicated by uncertainty whether earthquake loading or i.e. local sedimentation or scour was the agent. In depth analyses of all conditions affecting the submarine slope is then required. Where a large historical earthquake is known, the degree of burial of scars by subsequent sedimentation can sometimes provide the information to establish a connection between certain scars and the seismic event. Sometimes scars can be shown to be formed by anything but a large earthquake given even extremely conservative soil strength parameters. In seismically active areas, where seismicity is the likely trigger for instabilities, the frequency of scar formation can be derived from the distribution of post-failure sediment thickness over the scars in combination with information on sedimentation rate.

In most other cases direct indications on the effects of seismicity on offshore slope stability cannot be given.

Analyses of earthquake induced offshore slope stability hazards then has to refer to general conservative estimates of bulk soil property conditions and build up. In general, such estimation requires a geological analysis of the region of the slope to enable determination of the build up, and indications on the type of soils involved. The types of soils and properties are determined from sedimentary facies, or from simple correlation with Atterberg limits *et cetera* if sufficient samples are available.

The quantitative uncertainties in seismic hazard analyses together with the quantitative uncertainties in soil build up and properties, soon lead to unacceptable risk levels if fully quantitative stochastic modeling is used. Bounds from deterministic reasoning can sometimes be formulated, but very often, the less formally derived expert opinion has to be invoked to come to reasonable hazard level assessments in offshore earthquake induced slope stability hazard assessment.

1.6. Sub-surface properties

For all calculations or estimates of on-and offshore slope stability, sub-surface properties of the soil or rock mass have to be known. In many cases, these will not be the same as the mass properties at the time when the slope stability calculation is made. All materials weather with time mostly leading to a deterioration of strength characteristics, with a weathering rate depending on environment, such as climate, groundwater, man-made use of the ground, etc. In some situations a major deterioration of the strength characteristics of a mass may happen in a couple of years while for others it may take millions of years before a notable change in mass strength characteristics is observed. Most slope stability forecasting is done with an assumed validity of some 50 to 100 years in the future, which is generally the engineering lifetime of a civil engineering structure. Mostly a reasonable guess can be made how a soil or rock mass behaves for long (geological-) times and mostly intact material properties can be estimated from the behavior of gravestones or building stones. However, very little is known on the strength and deformation properties of a soil or rock mass in 50 to 100 years (Rengers et al., 2001).

2. Roermond earthquake, The Netherlands

On April 13, 1992, the southern parts of the Netherlands experienced an earthquake of magnitude 5.8 on the Richter scale. Twenty-five kilometers from the epicenter two landslides occurred during, or shortly after this event in an area called the Brunssummer Heide. A field survey was carried out (Alkema et al., 1994) to reconstruct the mechanics of the destabilization. No direct measurements of ground acceleration during the earthquake were available at the Brunssummer Heide. Estimates of the peak ground acceleration were based on different empirical attenuation relationships (e.g. Campbell, 1981; Chiaruttini and Siro, 1981; Joyner and Moore, 1981; Campbell, 1985; Joyner and Moore, 1988; Ambraseys, 1990) and ranged from 0.05 g to 0.14 g. Ahorner (1992) proposes to use the empirical formula of Joyner and Moore (1981) that results in a peak acceleration of 0.07 g.

2.1. Liquefaction susceptibility

The material in which the landslides occurred consists of well-sorted fine-grained sands with 90% of the grains between 100 and 200 μm of the Pleistocene Heksenberg formation. This particular grain size distribution is generally considered highly susceptible to liquefaction. Several samples were subjected to consolidated drained triaxial tests. The results showed that no significant difference exists between peak and residual strength. The angle of internal friction (φ') was determined at 33° with no cohesion. At the sites of both landslides, no clear morphological features were found that would indicate liquefaction phenomena. However, at a distance of several hundred meters, possible ground subsidence was observed and further away (several kilometers) remains of sand volcanoes were found. These features may indicate that liquefaction phenomena may have occurred in at least part of the formation. The liquefaction susceptibility of a saturated deposit depends on the ability to densify during shaking and the potential for pore pressure increase caused by this densification. Youd and Perkins (1978) give a threshold magnitude 6.7 for an earthquake to cause liquefaction at a distance of 25 km from the epicenter. They also state that liquefaction in deposits older than the Pleistocene is not likely to occur because they are already well consolidated. However, the sands at the location of the landslides seem to have been reworked in the last centuries during surface lignite mining.

2.2. Stability analysis

Cross section profiles were made for both landslides to enable reconstruction of the original slope surface and the most probable plane of failure. The groundwater table at the time of the earthquake was considered three meters below the surface. This was based upon

observations immediately after the event and on the rainfall data from before the event. The stability of the slopes is expressed with the safety factor (F) that is defined as: F = available shear strength / shear stress, similar to Eq. (1). Several methods of slope stability analysis exist. The results presented here are based on the simplified method of Janbu with the Fredlund correction (Fredlund, 1974). The safety factors for the original slopes are 3.0 and 2.6 respectively. Even with the groundwater table at the surface, both slopes would have remained stable with safety factors of respectively 1.5 and 1.2. With no pore water increase, a horizontal acceleration of minimal 0.3 g would be necessary to destabilize both slopes. This seems unlikely because the peak ground acceleration based on the empirical attenuation relationships ranged from 0.05 to 0.14. To cause slope failure with these accelerations, a pore pressure increase of 100% for a_{max} = 0.14 g is needed and more than 200% for a_{max} = 0.05 g.

The pore pressure increase is caused by the cyclic loading at the plane of failure or by dissipation of increased pore pressure from a deeper liquefied zone. The study of Alkema et al. (1994) gives lower limit values of the pore pressure increase, because it was assumed that the peak ground acceleration and the maximum reduction of effective normal stress coincide in time, which is not necessarily true. Furthermore, it became apparent that little or no information existed on attenuation relationships in Northwest Europe.

3. Umbria–Marche earthquake of 26 September 1997

A seismic sequence of moderate magnitude that started on September 26th 1997 struck the Umbria–Marche area, in central Italy (Fig. 3). On September 26th a shock of M_w 5.7 occurred at 00.33 GMT and was followed by a stronger earthquake of M_w 6.0, at 9.40 GMT, which represents the main shock of the entire sequence (Amato et al., 1997). Lately, on October 14th, an earthquake of M_w 5.7 occurred at 15.23 GMT, in an area located to the SE (Fig. 3). These shocks induced several mass movements that affected a large variety of geological formations of the Umbria–Marche stratigraphic sequence, made of limestone, marly limestone, marls and flysch sequences. The landslides also affected some of the quaternary soils such as the stratified periglacial deposits on calcareous slopes, the colluvial deposits on flysch formations, and the alluvial terraces and travertines.

Two sets of landslides were identified during aerial photo interpretation and fieldwork. The first set consists of landslides caused by the main shock in the northern part of the area, and consists of soil and dry debris slides on colluvial soils and stratified periglacial deposits. These have been utilized to test the validity of the empirical laws that calculate the displacement of landslides occurring along a failure surface. The second set consists of landslides caused by the shock of October 14 and are rock

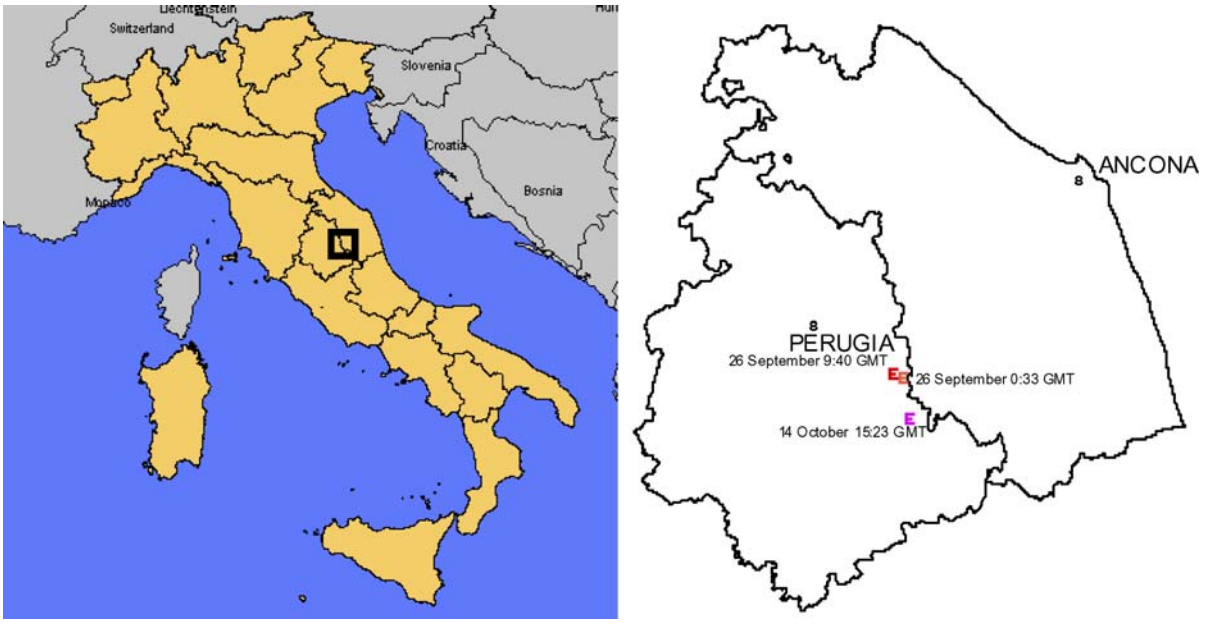

Fig. 3. Location of the Umbria–Marche earthquake and sequence of shocks.

falls on calcareous formations. This gave the opportunity to explore the relation existing between landslide occurrence, morphologic characteristics of the slope, and strong ground motion parameters.

3.1. Mass movements along failure surfaces

The landslide displacement along the failure surface is based on the theory proposed by Newmark (1965). It simplifies the landslide as a rigid block that slides along an inclined surface. The boundary between failure surface and block behaves rigid-plastically and under a cyclic load applied at the base, the displacement occurs whenever the acting shear stress exceeds the resistance strength. Newmark's model has been generalized by various authors in the form of empirical laws that calculate the displacement in function of the landslide susceptibility to failure and the strong ground motion parameters, such as Peak Ground Acceleration (PGA), Peak Ground Velocity (PGV), etc. The landslide susceptibility to failure is generally expressed by the critical horizontal acceleration, that is the minimum amount of acceleration that can bring the slope to the limit equilibrium and accounts for slope geometry, geotechnical properties of soils and hydro-geologic conditions. The empirical relationships conform to the general form of Eq. (2):

$$f(D) = A \cdot g(s) + B \cdot h(k) + C$$
D = the landslide displacement; $g(s)$ = the seismic parameter
$h(k)$ = the landslide susceptibility to failure; A, B, C = constants (2)

Four empirical rules based on different strong ground motion parameters of different accelerometer recordings, have been applied to the same data set, in order to verify their accuracy. Ambraseys and Srbulov (1995) proposed the simplest rule, where displacement depends on earthquake magnitude and distance from the hypocenter. Jibson et al. (1998) and Romeo (1998) proposed two rules both based on the Arias Intensity parameter, but obtained from two different strong motion sets. Finally Crespellani et al. (1998) proposed a rule based on the Destructiveness Potential.

The comparison has been carried out with the aid of a Geographic Information System (GIS), used for map storage and analysis. The analyses consisted of four steps: a) a landslide susceptibility map was created, expressed in the K_c parameter; b) the earthquake parameters were calculated; c) calculation of the displacement map applying the empirical rules; d) test of prediction performance by overlaying the predicted displacement to the actual landslides (Luzi and Pergalani, 2000).

Among the validation techniques existing in the literature, it was preferred to apply the one proposed by Chung and Fabbri (1997). It assumes that the best method is the one that can predict the highest number/percentage of occurred landslides in the smallest amount of hazardous area (the displaced pixels). The Umbria–Marche data set indicates that the rule based on the Destructiveness Potential (P_D) parameter works quite well and can correctly predict up to 70% of landslides that have occurred during the September 26 earthquake (Fig. 4). The equation is of the following form:

$$D_n = 0.021 P_D^{0.910} \cdot K_c^{-1.202}$$
D_n = displacement (cm); P_D = Destructiveness Potential(10^{-3} g s^3)
K_c = critical horizontal acceleration coefficient (3)

No control for the relative values $K_c - PGA$ is requested. The standard deviation of D_n is 0.746, while the coefficient of correlation (R2) is 0.889. Correction

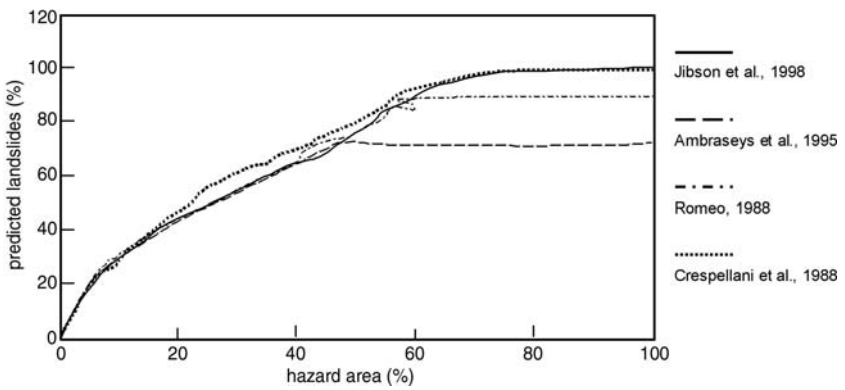

Fig. 4. Results of the accuracy test of the empirical laws based on Newmark's theory.

factors should be applied to the final displacement outcome when considering planar or rotational landslides. There is no considerable difference when using the Destructiveness Potential instead of the Arias Intensity (Fig. 4), therefore it is advisable to use this second parameter that is far easier to estimate, even using the common attenuation laws for strong motion parameters proposed in literature.

3.2. Rock fall landslides

The data set of rock falls that occurred on October 14 was used to formulate an empirical law in the form of Eq. (2) that could set up a relation among rock falls and triggering parameters. It was initially supposed that the main triggering factors should be: lithology, slope angle, and strong ground motion parameters. Therefore, the variability of these parameters and the distribution of detachment areas in the territory had to be determined. A task easily achieved with the aid of a GIS. A dependent variable was associated with the relative density of landslides for every combination of the triggering factors, obtained by map overlay and simple statistics. The relative density of landslides also quantifies the landslide hazard, thus represented in terms of failure probability. The limitation of the approach is, of course, the neglecting of the size and run out path of boulders.

Several linear regression formulas have been attempted in order to select the most favorable one, as well as several strong ground motion parameters, such as peak ground acceleration, Arias Intensity and Peak Ground Velocity, usually assumed as the parameter better correlated with rock falls. The Umbria–Marche data set indicated that the parameter best correlated with the rock fall occurrences is the PGA. The obtained rule

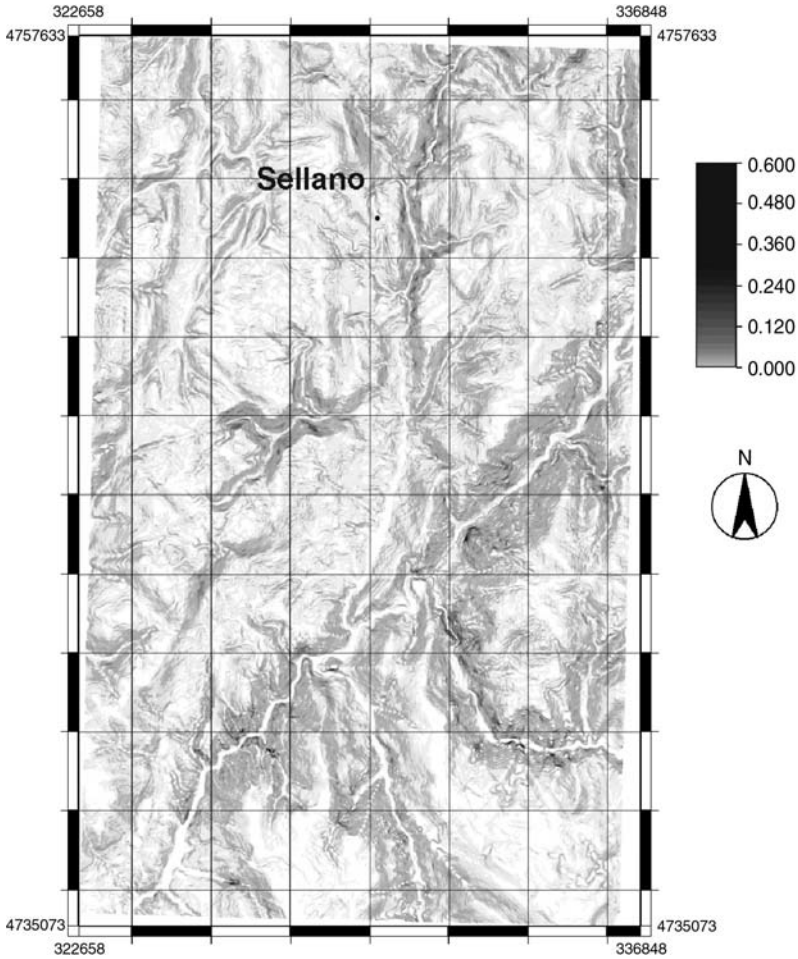

Fig. 5. Example of application of Eq. (3) on the Umbria–Marche data set (the pixel values indicate the probability of failure).

has the following form:

$$\log \mathrm{Dr} = 0.056575\ S + 0.670365\ \mathrm{PGA} - 4.565747$$

Dr = the relative density of landslides, S = the slope angle
PGA = the Peak Ground Acceleration

(4)

The standard deviations of Dr, S, PGA, and of the constant are respectively 0.331165, 0.001035, 0.056624, and 0.064653, while the coefficient of correlation (R^2) equals 0.87. The geology data layer has been discarded because of the strict correlation with slope angle, therefore only one of the two layers is required for the statistical analysis.

A practical example of a hazard map, obtained by applying Eq. (3) to the same data set with which it was obtained, is shown in Fig. 5; the values in the map indicate the probability of rock block detachment. The actual accuracy of Eq. (3) needs to be tested with other data sets and a possible development may be the use of the rock fall landsides caused by the Friuli earthquake of May 1976.

4. Three-dimensional site-effects during the Armenia earthquake of January 1999

On January 25, 1999, an earthquake of magnitude 6.2 on the Richter scale caused considerable damage in the Coffee region of Colombia, which is part of the Andes mountain range. The earthquake caused more than 900 casualties, at least 4000 people were injured, and some 200,000 citizens were left without shelter (El Colombiano, 1999). The epicenter of the earthquake was located about 15 km south of Armenia (Fig. 6). In Armenia (about 250,000 inhabitants), the damage was extensive and large parts of the city were destroyed. In Armenia no accelerogram of the earthquake itself was recorded, but based on recordings from nearby accelerograph stations, and back analyses of after shocks, the horizontal and vertical peak ground accelerations on horizontal and flat soil surfaces were estimated. Horizontal and vertical acceleration were estimated to have reached maximum values of 0.59 g respectively 0.47 g (Ingeominas, 1999).

4.1. Crocodile effect

In the context of a project for reconstruction of Armenia (Hack, 2000; Slob et al., 2002), it became apparent that site effects had been of major influence on the damage pattern. Near slopes, the effect was stronger than expected, which was assumed to be due to the nature of the specific topography. Part of the city of Armenia is built on ridges with relatively deep and steep valleys in-between. The top of the ridges is about flat. The width of the ridges reduces from east to west. On some of the ridges, a fairly sharp boundary line perpendicular to the ridge seemed to indicate a change in damage pattern.

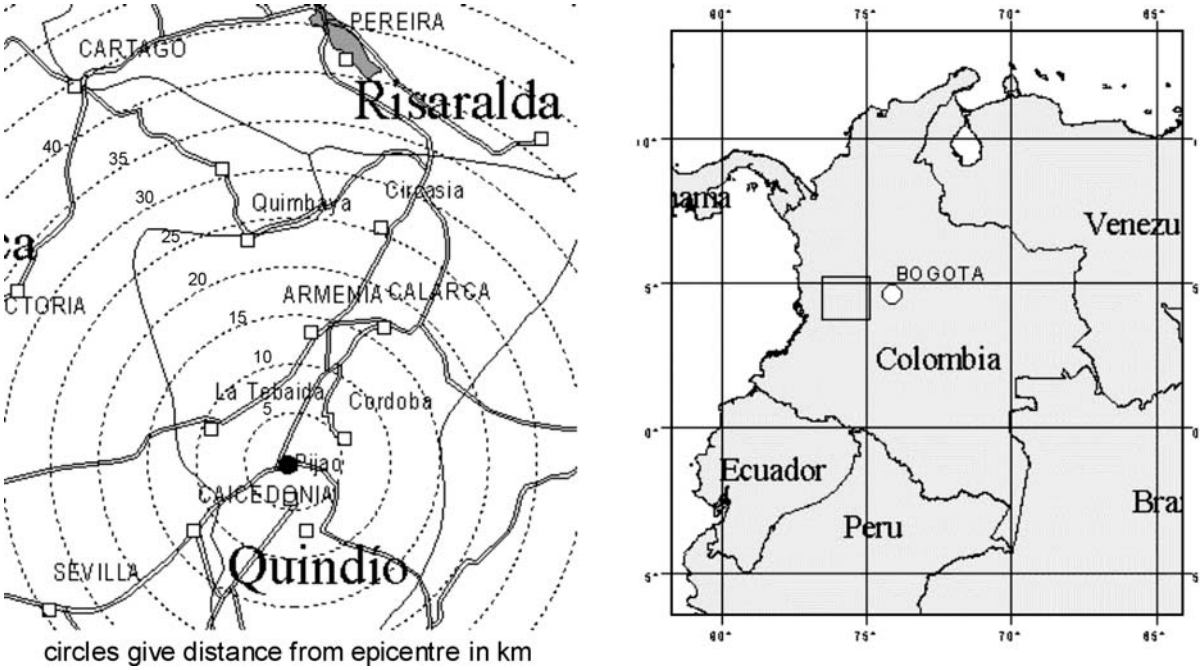

Fig. 6. Epicenter of the 1999 Armenia earthquake (after Ingeominas, 1999).

Damage to houses on the ridge where the ridge had a width wider than at the boundary line was limited while destruction was near to complete on the other side of the boundary. Neither the type nor the quality of the structures and houses was noticeably different on both sides of the boundary. Also no changes in subsoil material or in the depth of bedrock were known that could explain the existence of this fairly sharp boundary line. Near to a slope edge, the accelerations can be expected to be higher than on a flat topography. This could be part of the explanation. At a certain width of the ridge, the slope effects from both sides of the ridge overlap and damage increases. However, the change in damage was so abrupt that just slope effects from both sides of the ridge were not thought to be enough to explain the sharp difference in damage on both sides of the boundary. Some form of a three-dimensional resonance effect had likely occurred in the ridges during the earthquake in which the accelerations increased from the wider to the more narrow part of the ridges. As the geometry of the topography of the ridges resembles the geometry of the tail of a crocodile and the movements of the tail of a fast moving crocodile is not un-similar to the assumed movements of the ridge during an earthquake, the effect was named "crocodile effect".

4.2. Numerical modeling

To investigate the validity of the hypothesis of the crocodile effect a three-dimensional numerical finite element model has been analyzed for the ridges (Leenders, 2000; Leenders and Hack, in preparation). As an example, a ridge in the Brasilia Nueva area of Armenia is modeled. The bedrock forms the bottom of the numerical model, overlain by a horizontal layer of 40 m of pyroclastic and lahar deposits followed by a layer of maximum 60 m thickness of only pyroclastic deposits. The "Modified Mohr–Coulomb" model (Desai and Abel, 1972), which combines a non-linear elastic or plastic deformation model with a failure surface model, is used as constitutive model for all layers. The model is made in DIANA (1998). The base of the model is subjected to the accelerations from a synthetic base accelerogram. Obviously, this is a strongly simplified model of reality (Fig. 7), but is acceptable for this demonstration study.

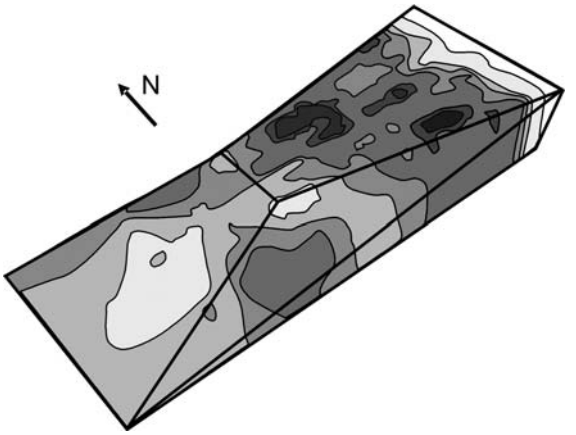

Fig. 8. Surface acceleration, from light to dark increasing surface acceleration (lightest 3 m/s^2 and darkest 17 m/s^2).

Fig. 8 shows the numerical modeling results. Only layer 2 is shown. The graying shows the different accelerations at surface. The darkest areas have peak acceleration in the order of 17 m/s^2 while the lightest areas have peak accelerations in the order of 3 m/s^2. The maximum acceleration increases indeed in the direction of the smaller part of the top of the ridge as expected. The pattern of maxima and minima as shown in Fig. 8 cannot be completely explained. More research has to be done to investigate this.

5. Conclusions and discussion

Although the behavior of a slope during an earthquake appears to be fairly well understood, in practice it works out to be rather complicated. Simple assumptions are often not enough to explain real behavior during an earthquake. In the forgoing examples, this is shown by the sometimes unexpected and may be strange results.

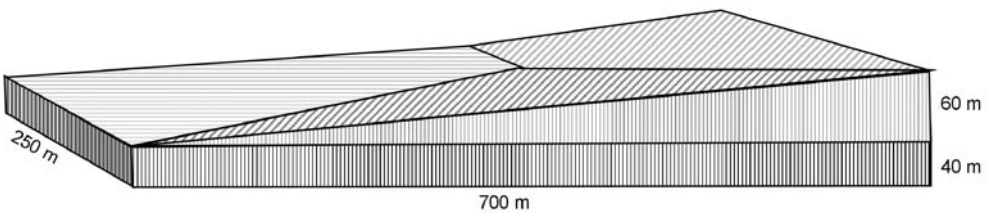

Fig. 7. Geometry of numerical model.

An increase of 100 to 200% in pore pressure as required explaining the slope instability in the case of the Roermond earthquake may happen, but is large. The result that geology is not important in the prediction of rock-falls in the Umbria–Marche earthquake seemed also strange. Unavailability or inaccuracy of data of the actual movements during the earthquake and lack of accurate sub-surface geotechnical data may have caused this. The Armenia case shows that highly complicated three-dimensional movements may explain damage patterns that cannot be explained by one or two-dimensional analytical or numerical calculations. Off-shore the problem of lack of data is obviously far more emphasized due to the limited accessibility to data and the impossibility to "see" what has happened. Always it should be realized that changes in the sub-surface materials, such as weathering, or in the use of the surface or ground are mostly the cause for slope instability with the earthquake only being the trigger. This means that accurate data has not only to be available, but should be of relatively recent date to be useful.

In foundation engineering similar observations have been made. After many earthquakes, it has been found that the buildings and foundations suffered damage more than what should have happened based on theoretical calculations. Therefore, after virtually each earthquake the required design calculation models are made more complicated, more sub-surface data are required, and the minimum required design safety factors are increased.

It can hence be doubted whether any simple assumption on the sub-surface geometry, variation of sub-surface materials, and/or simple calculation method are useful in earthquake engineering for slopes. The three-dimensional model shows that even for a simple geometry the pattern of acceleration is so complicated that prediction with a simple model seems to be senseless.

References

Ahorner, L., 1992. Gemessene Bodenbeschleunigungen beim Roermonder Beben am 13. Bauingenieur 68, 201–205 (April).

Alkema, D., Mosselman, M., Paulussen, I., 1994. Earthquake triggered landslides at the Brunssummer Heide, Limburg, the Netherlands: preliminary studies following the 1992 Roermond earthquake. Geologie en Mijnbouw, vol. 73. Kluwer Academic Publishers, the Netherlands, pp. 387–391.

Amato, A., Azzara, R., Basili, A., Chiarabba, C., Cimini, G.B., Cocco, M., Di Bona, M., Margheriti, L., Mazza, S., Mele, F., Selvaggi, G., Boschi, E., Bittarelli, G., Chiaraluce, L., Piccinini, D., Ripepe, M., Courboulex, F., Deschamps, A., Gaffet, S., 1997. Studio sismologico preliminare della sequenza di Colfiorito. Studi preliminari sulla sequenza sismica dell'Appennino Umbro-Marchigiano del Settembre 1997.

Ambraseys, N.N., 1990. Uniform magnitude re-evaluation of European earthquakes associated with strong-motion records. Earthq. Eng. Struct. Dyn. 19, 1–20.

Ambraseys, N., Srbulov, M., 1995. Earthquake induced displacement of slopes. Soil Dyn. Earthqu. Eng. 14, 59–71.

Anon, 1997. Report on Early Warning Capabilities for Geological Hazards. Convener of International Working Group, and first author: Dr. Robert Hamilton Chairman, International Decade for Natural Disaster Reduction (IDNDR). Early Warning Programme, IDNDR Scientific and Technical Committee Washington, D.C. USA. document 12085, IDNDR Secretariat, Geneva. 35 pp.

Boulanger, R.W., Bray, J.D., Merry, S.M., Mejia, L.H., 1995. "Three-Dimensional Dynamic Response Analyses of Cogswell Dam," Canadian Geotechnical Journal, Vol. 32, No. 3, pp. 452–464, June, 1995, which is based on: Boulanger, R. W., Merry, S. M., Bray, J.D., and Mejia, L. (June 1994). "Dynamic Response Analyses of Cogswell Dam During the 1991 Sierra Madre and 1987 Whittier Narrows Earthquakes", Geotechnical Engineering Report, University of California at Davis.

Campbell, K.W., 1981. Near-source attenuation of peak horizontal acceleration. Bull. Seismol. Soc. Am. 71, 2039–2070.

Campbell, K.W., 1985. Near-source attenuation of strong ground motion for the Eastern United States. Second Quarter Progress Report FY 1985 to the U.S. Nuclear Regulatory Commission, pp. 1–14.

Chiaruttini, C., Siro, I., 1981. The correlation of peak ground horizontal acceleration with magnitude, distance and seismic intensity for Friuli and Ancona, Italy and the Alpine Belt. Bull. Seismol. Soc. Am. 71, 1993–2009.

Chung, C.J., Fabbri, A.F., 1997. Sensitivity analysis of quantitative prediction models based on map overlays: an application to landslide hazard zonation. IV Int. Congr. On Geomorphology, Bologna, Italy, August 28– September 3, 1997.

Crespellani, T., Madiai, C., Vannucchi, G., 1998. Earthquake destructiveness potential factor and slope stability. Géotechnique 48 (3), 411–419.

Desai, C.S., Abel, J.F., 1972. Introduction to the Finite Element Method. A numerical Method for Engineering Analysis. Van Nostrand, New York. 477 pp.

DIANA, 1998. In: Witte, F.C. (Ed.), DIANA-Finite Element Analysis, User's Manual release 7, TNO DIANA. TNO Building and Construction Research, Delft, The Netherlands.

Fredlund, D.G., 1974. Slope Stability Analysis, Users Manual, Fellenius or Ordinary Method, Simplified Method, Spencers Method, Janbus Simplified Method, Janbus Rigorous Method, Morgenstern-Price Method. CD-4 Report, Transportation and Geotechnical Group. University of Saskatchewan, Saskatoon, Saskatchewan.

Hack R. (Ed.) (2000) Rapid Inventory of Earthquake Damage (RIED) Assessment of the damage of the Quindío Earthquake in Armenia and Pereira, Colombia. Unpublished report, March 2000, ITC, Delft, The Netherlands. 140 pp.

Harris, G.M., Beardow, A.P., 1995. The destruction of Sodom and Gomorrah: a geotechnical perspective. Q. J. Eng. Geol. 28 (4), 349.

Hatzor, Y.H., Goodman, R.E., 1997. Three dimensional back analysis of saturated rock slopes in discontinuous rock—A case study. Geotechnique 47 (4), 817–839.

Hubbert, M.K., Rubey, W.W., 1959. Role of fluid pressure in mechanics of overthrust faulting. Bull. Geol. Soc. Am. 70, 115–166.

Ingeominas, 1999. Terremoto del Quindio, Enero 25 de 1999, Informe Technico Cientifico. Ingeominas, Santa Fe de Bogota, Colombia. Web published report http://productos.ingeominas.gov.co. 34 pp.

Ishihara, K., 1986. Stability of natural deposits during earthquakes. collected papers, vol. 24. Dept. Civil Eng, Tokyo, pp. 1–56.

Jibson, R.W., Harp, E.L., Michael, J.A., 1998. A method for producing digital probabilistic seismic landslide hazard maps: an example from the Los Angeles, California, area. US Geological Survey O-F Report, pp. 98–113.

Joyner, W.B., Moore, D.M., 1981. Peak horizontal acceleration and velocity from strong-motion records including records from the 1979 Imperial Valley, California, Earthquake. Bull. Seismol. Soc. Am. 2011–2038.

Joyner, W.B., Moore, D.M., 1988. Measurement, characterization and prediction of strong ground motion. Proc. Earthquake Engineering and Soil Dynamics II, GT Div/ASCE, Park City, Utah, June 27–30, pp. 43–102.

Khazai, B., Sitar, N., 2000. Assessment of seismic slope stability using GIS modeling. Geogr. Inf. Sci. 6 (2) (December).

Kramer, S.L., 1996. Geotechnical earthquake engineering. Publ. Prentice-Hall Inc. 653 pp.

Leenders, A.G., 2000. Three-dimensional dynamic modelling of earthquake tremors. Memoirs of the Centre of Engineering Geology in The Netherlands. 1386-5072, vol. 200. Faculty of Civil Engineering and Geoscience, Department of Applied Earth Sciences, Division Engineering Geology, Technical University Delft, The Netherlands. August, 64 pp.

Leenders, AG, and Hack, H.R.G.K. (in preparation) Three-dimensional dynamic modelling of resonance effects during earthquake tremors.

Luzi, L., Pergalani, F., 2000. A correlation between slope failures and accelerometric parameters: the 26 September 1997 earthquake (Umbria–Marche, Italy). Soil Dyn. Earthqu. Eng. 20, 301–313.

Newmark, N.M., 1965. Effects of earthquakes on dams and embankments. Geotechnique 15 (2), 139–160.

Nova-Roessig, L., Sitar, N., 1998. Centrifuge studies of the seismic response of reinforced soil slopes. Proceedings of the Third Geotechnical Engineering and Soil Dynamics Conference. Geotechnical Special Publication, vol. 75. ASCE, Seattle, Washington, pp. 458–468. August 3–6.

Prakash, S. (Ed.), 2001. Proc. Fourth International Conference on Recent Advances in Geotechnical Earthquake Engineering and Soil Dynamics, San Diego, CA. March 26–31.

Rathje, E.M., Bray, J.D., 2001. One- and two-dimensional seismic analysis of solid-waste landfills. Can. Geotech. J. 38 (4), 850–862 (August).

Rengers, N., Huisman, M., Hack, H.R.G.K., Rupke, J., 2001. Quantification of engineering geological parameters — GIS-based slope instability hazard and risk assessment. 50th Geomechanics Colloquium, October, 2001, Salzburg, Austrian Society for Geomechanics. Felsbau, 19, nr. 5, pp. 102–106.

Romeo, R., 1998. Seismically-induced landslide displacements: a predictive model. XXIII General Assembly of European Geophysical Society, Nice.

Slob, S., Hack, R., Scarpas, T., Van Bemmelen, B., Duque, A., 2002. A methodology for seismic microzonation using GIS and SHAKE—a case study from Armenia, Colombia. In: van Rooy, J.L., Jermy, C.A. (Eds.), Engineering Geology for Developing Countries—Proceedings of 9th Congress of the International Association for Engineering Geology and the Environment. Durban, South Africa, 16– 20 September 2002, pp. 2843–2852.

Terzaghi, K., 1950. Mechanism of landslides. In: Paige, S. (Ed.), Application of geology to engineering practice (Berkey Volume). Geological Society of America, New York, pp. 83–123.

Youd, T.L., Perkins, D.M., 1978. Mapping liquefaction induced ground failure potential. J. Geotech. Eng. Div. ASCE 104, 433–446.